Determining the parameters of demarcation of heat exchange modes in the film during vaporization

Valentyn Petrenko, Oleksiy Pylypenko, Oleksandr Ryabchuk, Maksym Nalyvaiko

National University of Food Technologies, Kyiv, Ukraine

Keywords:

Heat exchange
Film
Liquid
Temperature
Turbulence
Velocity

Article history:

Received 30.11.2022
Received in revised form 3.03.2023
Accepted 31.03.2023

Corresponding author:

Valentyn Petrenko
E-mail: ufi_nuft@meta.ua

DOI: 10.24263/2304-974X-2023-12-1-9

Abstract

Introduction. The purpose of the research is to analytically determine the parameters of the separation of two characteristic modes of heat transfer to the boiling film under the condition of its cyclic mixing by large waves, which takes place in the long pipes of film evaporators of the sugar industry.

Materials and methods. Analytical methods of analysis of heat transfer processes in flowing laminar and turbulent films of liquids during vaporization are applied in the study.

Results and discussion. Mathematical modeling of the temperature field in a liquid flowing down the vertical surface of a boiling film with a developed wave structure in the presence of an accompanying vapor flow at the time of the appearance of a temperature gradient at the film-vapor interfacial surface was carried out. The perturber of cyclic temperature fluctuations in the film in long channels are large low-frequency waves that roll along the interfacial surface. The limiting curve for separating heat transfer modes in the film is obtained on the basis of the approximate solution of the differential equation of heat conduction with a convective term for both laminar and turbulent modes of film motion using the algebraic form of dependence for turbulent viscosity in the film provided under the condition of zero temperature gradient on the surface of the film. As a result of solving the problem, an analytical expression was obtained, which is the initial condition of the boundary value problem of heat transfer in a boiling film, which arises at the moment of stirring the film by a large wave. It was found that with a change in the volume density of irrigation from 0.0001 to 0.0005 m^2/s, the length of the film run, during which the heat exchange mode changes, is 50–140 mm for laminar films and 10–35 mm for turbulent films, respectively.

Conclusions. From the equations of convective heat conduction for laminar and turbulent films under the condition of zero temperature gradient on the surface of the film, expressions are obtained that are the initial conditions of the boundary value problem of heat exchange in a boiling film, which occurs at the time of mixing of the film by a large wave.

Introduction

Transfer processes in flowing films of liquids with interaction with a gas (vapor) flow are characterized by high intensity due to the powerful interaction of the gas flow with the surface of the film covered by a complex system of surface waves. In addition, film processes are fast-moving, which is especially important in the processes taking place in heat and mass exchange devices of the food industry, where the determining factor in improving the quality of products during their heat treatment in evaporation devices is a short stay in the zone of elevated temperature.

Considering the variety and complexity of the structural forms of surface waves, which have a decisive influence on the intensity of transfer processes in films, a large number of works are devoted to the study of wave characteristics of films and modeling of thermal-hydrodynamic processes in films. But the majority of them are devoted to the analysis of thermohydrodynamic processes in films on short sections of pipes, where the wave structure is formed by a system of high-frequency capillary waves on the surface of laminar films of water (Dietze et al., 2014; Lel et al., 2015) and viscous liquids (Gourdon et al., 2015). Turbulence in films has also been studied on short sections and has a specific structure associated with the damping of turbulent pulsations by the interfacial surface (Mascarenhas et. al., 2013). There is a limited number of experimental and theoretical works on the study of heat transfer and hydrodynamics of film flows in long pipes, where the structure of large low-frequency waves is formed (Kostoglou et al., 2010; Malamataris et al., 2008). However, the large waves that are formed at a distance of 1.5–3 m from the entrance play a decisive role in the processes of heat exchange in long steam-generating channels. Since the speed of the large waves exceeds the speed of the interphase surface of the film (by 2.5–1.5 times depending on the Re number), and their amplitude is 2–3 times greater than the average thickness of the film, deformed large waves act on the film like a bulldozer, rolling over the interfacial surface. It was established that a large wave during its movement has a central vortex (Demekhin et al., 2005), due to which the film is mixed during its movement of the wave. Taking into account the above, the following mechanism of heat exchange in the presence of large waves appears: at the moment of the passage of a large wave, the mass of liquid superheated relative to the saturation temperature moves from the wall layer to the interphase surface, where, as a result of self-evaporation, it cools to the saturation temperature. In the time interval between the passage of two large waves, two successive processes take place: the first begins immediately after mixing the film and continues until the state when the temperature wave reaches the interphase surface; the second begins from the moment of the appearance of a positive temperature gradient on the interphase surface and, accordingly, is manifested by the beginning of evaporation. The intensity of evaporation increases with the growth of the temperature gradient on the interfacial surface and this process continues until the next big wave passes. The limit state of the heating of the film in the second period is a temperature curve that corresponds to the steady mode of heat exchange, but this state, due to the significant frequency of passing waves (7–10 *Hz*), is not reached.

Thus, taking into account the development of the temperature field along the surface of the heat exchange, the temperature profile in the period between the passage of large waves can be obtained from the equation of convective heat conduction, in which, under the laminar regime of motion of the film, the convective term is written in the form of a parabolic velocity profile

$$\left[\left(\frac{\tau_i}{\rho\nu}+\frac{g\,\delta}{\nu}\right)y-\frac{g}{2\,\nu}y^2\right]\frac{\partial\,t(x,y)}{\partial x}=a_l\,\frac{\partial^2 t(x,y)}{\partial y^2}, \tag{1}$$

and for turbulent – in the form of a power equation:

$$u_i\left(\frac{y}{\delta}\right)^{1/n}\frac{\partial t(x,y)}{\partial x}=\frac{\partial}{\partial y}\left(a_l+a_t\right)\frac{\partial t(x,y)}{\partial y}, \tag{2}$$

where x and y are the longitudinal and transverse coordinates, respectively; τ_i is a shear stress on the interfacial surface of the film; t is a temperature; δ is an average film thickness; ν,ρ – kinematic viscosity, liquid density, respectively; g – acceleration of free fall; u_i – velocity of the liquid in the film on the interfacial surface; a_l, a_t – molecular and turbulent thermal conductivity, respectively.

The exponent n varies from 1/5 to 1/7 depending on the Reynolds number (irrigation density). Turbulent thermal conductivity a_t, which is included in equation (2), is determined through turbulent viscosity ν_t, since these parameters are related by the equation

$$\frac{a_t}{a_l}=\frac{\nu_t}{\nu}\frac{\Pr}{\Pr_t},$$

where Pr, $\Pr_t$ are the molecular and turbulent Prandtl numbers, respectively.

A list of the main dependencies for the algebraic form of relations for turbulent viscosity in flowing films of liquids is given in (Mascarenhas et. al., 2013). Among the latest relations proposed in the literature for the algebraic form of turbulent viscosity for film flows with accompanying vapor flow in vertical evaporation channels is the relation (Petrenko et al., 2020)

$$\frac{\nu_t}{\nu}=5\cdot 10^{-5}\,\mathrm{Re}^{1,4}\left\{1+3,6\left[1-\exp\left(1-\frac{d}{d_o}\right)\right]\right\}f_u\eta^2\left(1-\eta^2\right), \tag{3}$$

where $f_u=C_u\left[1-0,1\exp\left(-1,1086\sqrt{We}\right)\right]$,

$$C_u=1,119-0,122\sqrt{We}+\left(0,07424+\frac{\mathrm{Re}}{9,153\cdot 10^6}\right)\left(\sqrt{We}\right)^2-0,01808\left(\sqrt{We}\right)^3+$$
$$+1,775\cdot 10^{-3}\left(\sqrt{We}\right)^4--7,8\cdot 10^{-5}\left(\sqrt{We}\right)^5+1,28\cdot 10^{-6}\left(\sqrt{We}\right)^6,$$

$We=\frac{\rho_2 u_2^2 d_o}{\sigma}$ – the Weber number; u_2 – steam core velocity; ρ_2 – density of steam; σ – surface tension; d_o= 0,02 *m*.

Ratio (3) is correct in the range $We \le 250$ for pipes with diameters from 20 to 32 *mm* (investigated range).

Graphical interpretation (3) for different phase costs is shown in Fig.1

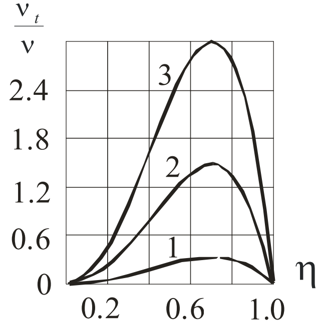

Figure 1. Dependence $\frac{\nu_t}{\nu} = f(\eta)$ on the ratio (3) for water at t = 100 ºC, d = 0,02 m and u_2 = 10 m/s;

1 – Re = 1356; 2 – 4068; 3 – 6780.

Boundary conditions (on the heat exchange wall ($y = 0$) and the interphase surface ($y = \delta$) for the first period: $y = 0$, $t = t_w$; $y = \delta$, $\frac{\partial t}{\partial y} = 0$ and initial conditions $x = x_m$, $t = t(x_m, y)$. For the second period, the boundary conditions are: $y = 0$, $t = t_w$; $y = \delta$, $t = t_{sat}$, and initial conditions $x = x_m$, $t = t(x_m, y)$. The index "*w*" refers to the wall, "sat" – the state of saturation; "m" corresponds to the transition conditions from period 1 to period 2. The function $t(x_m, y)$ is a solution of equations (1, 2) (depending on the mode of motion of the film) at the moment when $\frac{\partial t}{\partial y}\Big|_{y=\delta} = 0$. Equations (1, 2, 3) with the given boundary conditions make it possible to obtain the temperature distribution for both the first and second periods of the development of the temperature field in the film.

This work is devoted to the determination of the longitudinal coordinate x_m under which the condition is met $\frac{\partial t}{\partial y}\Big|_{y=\delta} = 0$ and the obtaining of the boundary temperature curve under these boundary conditions for laminar and turbulent films $t = t(x_m, y)$, which is the curve separating the two regimes of heat exchange in boiling films.

Materials and methods

The paper examines the parameters of distinguishing two modes of heat exchange in the model of heat exchange in boiling liquid films with a developed structure of large waves.

Research methods – analytical research based on the equations of convective heat conduction, using empirical coefficients in the ratio for turbulent viscosity, obtained based on the analysis of experimental data from the study of heat exchange processes in turbulent films (Petrenko et al., 2020).

The range of changes in regime parameters in which the obtained research results are correct is determined by the range of changes in parameters for which the empirical coefficients in the relation for turbulent viscosity were obtained (Petrenko et al., 2020) and is: the volumetric liquid flux varied in the range of 0,05–0,55x10^{-3} m^2/s. Steam speed 0–35 *m/s*, pipe diameter 20–34 *mm*; the length of the pipes is 1,5–9 *m*.

Results and discussion

Schematically, the temperature and velocity profiles in the film before and after the passage of a large wave are shown in Figure 2.

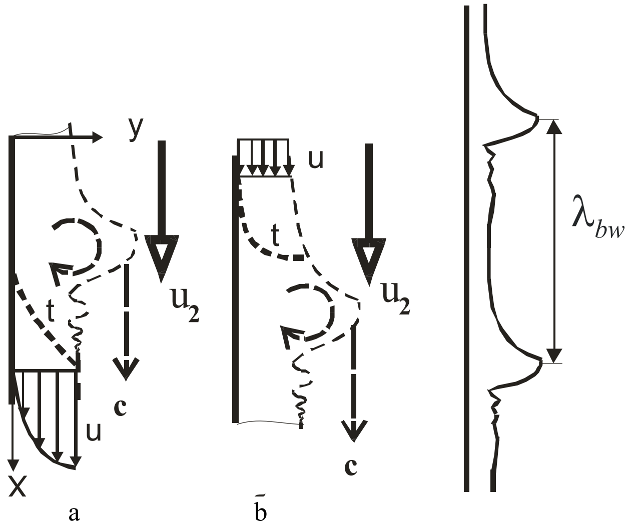

Figure 2. Scheme of the movement of a large wave on the surface of a turbulent film:
a – velocity and temperature profile before the passage of a large wave; b – after.
c – phase speed of large waves; λ_{bw} – length of large waves, accordingly.

Laminar mode of motion of the liquid film

We assume that in the laminar mode of motion at the time of appearance of the temperature gradient $\frac{\partial\theta}{\partial\eta}_{\eta=1}$ at the interphase boundary, the film travels the distance at which the velocity profile becomes parabolic or close to it. Then the convective heat transfer equation (1) in the presence of shear stress on the interphase surface τ_i in dimensionless form will be written as

$$\left[\left(\frac{\tau_i}{\nu\rho\delta}+\frac{g}{\nu}\right)\eta-\frac{g}{2\nu}\eta^2\right]\frac{\delta^3}{a_l}\frac{\partial\theta(\eta,\xi)}{\partial\xi}=\frac{\partial^2\theta(\eta,\xi)}{\partial\eta^2}, \tag{4}$$

where $\theta(\eta,\xi)=\dfrac{t(\eta,\xi)-t_{sat}}{t_w-t_{sat}}$ – the dimensionless temperature; $\eta=\dfrac{y}{\delta}$, $\xi=\dfrac{x}{\delta}$ – dimensionless transverse and longitudinal coordinates.

The task of finding the coordinate where the two modes of heat exchange in the film are separated during vaporization is formulated as follows. A liquid film flows down a vertical surface and is uniformly heated to the saturation (boiling) temperature t_{sat}. The temperature of the heat exchange surface, along which the film flows, instantly increases to t_w. Let's find the longitudinal coordinate ξ_m, or the distance covered by the film, at which the temperature profile will develop to the state at which a temperature gradient will appear on the interfacial surface of the film $\left.\dfrac{\partial\theta}{\partial\eta}\right|_{\eta=1}\geq 0$.

It can be solved (4) using an approximate method. To do this, replace the left part of (4) with the average value

$$\int_0^1\left[\left(\frac{\tau_i}{\rho\delta\nu}+\frac{g}{\nu}\right)\eta-\frac{g}{2\nu}\eta^2\right]\frac{\delta^3}{a_l}\frac{\partial\theta(\eta,\xi)}{\partial\xi}d\eta=\left(\frac{\tau_i\delta^2}{2\rho\nu}+\frac{g\delta^3}{3\nu}\right)\frac{1}{a_l}\frac{\partial\theta_{av}(\xi)}{\partial\xi}.$$

Given that the average speed is defined as

$$\bar{u}=\frac{1}{\delta}\int_0^\delta\left[\left(\frac{\tau_i}{\rho\nu}+\frac{g\delta}{\nu}\right)y-\frac{g}{2\nu}y^2\right]dy=\frac{\tau_i\delta}{2\rho\nu}+\frac{g\delta^2}{3\nu},$$

and the film thickness and the average velocity are related by a cubic equation

$$G_v=\bar{u}\delta=\frac{\tau_i\delta^2}{2\rho\nu}+\frac{g\delta^3}{3\nu}, \tag{5}$$

equation (4) takes the form

$$\frac{Pe}{4}\frac{\partial\theta(\eta,\xi)}{\partial\xi}=\frac{\partial^2\theta(\eta,\xi)}{\partial\eta^2}, \tag{6}$$

where $Pe=\dfrac{4G_v}{a_l}=\dfrac{4\bar{u}\delta}{a_l}$ – the Peclet number; G_v – volumetric liquid flux.

Double integration (6) under boundary conditions

$$\eta=0,\ \theta=1;\quad \eta=1,\ \frac{\partial\theta}{\partial\eta}=0, \tag{7}$$

gives

$$\theta(\eta,\xi)=\frac{Pe}{4}\frac{\partial\theta_{av}(\xi)}{\partial\xi}\left(\frac{\eta^2}{2}-\eta\right)+1. \qquad (8)$$

It was found the derivative $\frac{\partial\theta_{av}(\xi)}{\partial\xi}$ from the expression for the average temperature θ_{av}, which we give as mass average

$$\theta_{av}=\int_0^1\theta(\eta,\xi)\frac{u(\eta)}{\bar{u}}d\eta=\int_0^1\theta(\eta,\xi)\frac{\left[\left(\frac{\tau_i}{\rho\nu}+\frac{g\delta}{\nu}\right)\eta-\frac{g\delta}{2\nu}\eta^2\right]}{\left(\frac{\tau_i}{2\rho\nu}+\frac{g\delta}{3\nu}\right)}d\eta. \qquad (9)$$

Integration (9) gives

$$\theta_{av}=1-\frac{\partial\theta_{av}(\xi)}{\partial\xi}\frac{Pe}{80}\frac{25\tau_i+16\rho g\delta}{3\tau_i+2\rho g\delta}=1-\frac{\partial\theta_{av}(\xi)}{\partial\xi}D, \qquad (10)$$

where $D=\frac{Pe}{80}\frac{25\tau_i+16\rho g\delta}{3\tau_i+2\rho g\delta}$.

Integrating the differential equation (10) under the initial condition: $\xi=0$, $\theta_{av}=0$, we obtain an expression for the average temperature

$$\theta_{av}=1-\exp\left(-\frac{\xi}{D}\right). \qquad (11)$$

Differentiating (11) and substituting the derivative of (11) $\frac{d\theta_{av}(\xi)}{d\xi}$ into (8), we obtain the temperature distribution in the film at $\xi=\xi_m$, which is the boundary curve between the first and second characteristic regimes of heat exchange in the film

$$\theta(\eta,\xi_m)=\left(\frac{Pe}{4}\right)\frac{1}{D}\exp\left(-\frac{\xi_m}{D}\right)\left(\frac{\eta^2}{2}-\eta\right)+1. \qquad (12)$$

The graphic interpretation of (12) is shown in Figure 3.

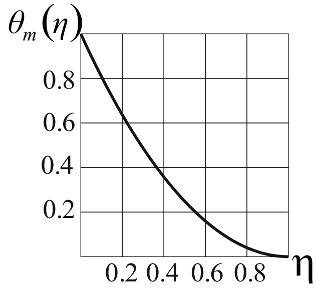

Figure 3. Graphic representation of the limiting temperature curve (12) at:
$Gv=0,5\cdot10^{-3}$ *m²/s*; $u_2=20$ *m/s*; $\tau_i=2,7$ *N/m*; $\delta=0,256\cdot10^{-3}$ *m*.

The coordinate ξ_m is determined from (12) under the condition that when $\xi = \xi_m$ the dimensionless temperature is zero, ($\theta(1, \xi_m) = 0$)

$$\xi_m = D \ln\left(\frac{Pe}{8D}\right). \tag{13}$$

With free flow ($\tau_i = 0$) $D = \frac{Pe}{80} \frac{25\tau_i + 16\rho g\delta}{3\tau_i + 2\rho g\delta} = \frac{Pe}{10}$, and the expression (13) for ξ_m takes the form

$$\xi_m = D \ln\left(\frac{Pe}{8D}\right) = \frac{Pe}{10} \ln\left(\frac{5}{4}\right) = 0,0223\, Pe. \tag{14}$$

Actual (physical) distance when defined as

$$x_m = \xi_m \delta .$$

The thickness of the laminar film during free flow on a vertical surface is defined as

$$\delta = \sqrt[3]{\frac{3 G_v \nu}{g}} ,$$

and in the presence of accompanying steam (gas) flow – as a result of solving the cubic equation (5). The results of dimensionless distance ξ_m and physical length x_m calculations for different vapor core velocities are shown in Figure 4.

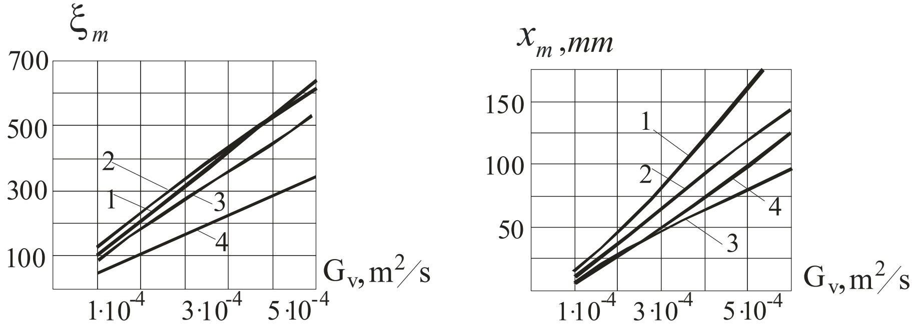

Figure 4. Dependence of the dimensionless ξ_m (a) and physical x_m (b) length overcome by a laminar film, at which the heat transfer regimes to the film change from the volumetric liquid flux G_v.

u, m/s: 1 – 15; 2 – 25; 3 – 35;
4 – free flow.

Turbulent mode of motion of a liquid film

For the turbulent motion of the film, we give the convective heat conduction equation (2) in dimensionless form

$$\frac{6\delta}{5}\bar{u}(\eta)^{1/5}\frac{\partial\theta(\xi,\eta)}{\partial\xi}=\frac{\partial}{\partial\eta}(a_l+a_t)\frac{\partial\theta(\xi,\eta)}{\partial\eta} \tag{15}$$

In relation (15), the power profile of the speed $u=u_i\eta^{1/n}$ is given by the average speed

$$u=u_i\left(\frac{y}{\delta}\right)^{\frac{1}{5}}=\frac{6}{5}\bar{u}\left(\frac{y}{\delta}\right)^{\frac{1}{5}}=\frac{6}{5}\bar{u}\,\eta^{\frac{1}{5}},\ \text{(at } n=1/5\text{)}.$$

By replacing the left side of equation (15) with the average value

$$\int_0^1\frac{6\delta}{5}\bar{u}(\eta)^{1/5}\frac{\partial\theta(\xi,\eta)}{\partial\xi}\partial\eta=\delta\bar{u}\frac{\partial\theta_{av}(\xi)}{\partial\xi},$$

we will get

$$\frac{Pe}{4}\frac{\partial\theta_{av}(\xi)}{\partial\xi}=\frac{\partial}{\partial\eta}\left(1+\frac{a_t}{a_l}\right)\frac{\partial\theta(\xi,\eta)}{\partial\eta}. \tag{16}$$

Since $\frac{a_t}{a_l}=\frac{\nu_t}{\nu}\frac{\mathrm{Pr}}{\mathrm{Pr}_t}$, expression (16) will be rewritten in the form

$$\frac{Pe}{4}\frac{\partial\theta_{av}(\xi)}{\partial\xi}=\frac{\partial}{\partial\eta}\left(1+\frac{\nu_t}{\nu}\frac{\mathrm{Pr}}{\mathrm{Pr}_t}\right)\frac{\partial\theta(\xi,\eta)}{\partial\eta}. \tag{17}$$

The boundary and initial conditions under which the boundary temperature curve in the film is located are similar to the laminar flow regime of the film (7)

$$\eta=0,\ \theta=1;\quad \eta=1,\ \frac{\partial\theta}{\partial\eta}=0;\quad \xi=0,\quad \theta=0.$$

Integrating (17) under the condition $\eta=1$, $\frac{\partial\theta}{\partial\eta}=0$, gives

$$\theta(\eta,\xi)=\frac{Pe}{4}\frac{\partial\theta_{av}(\xi)}{\partial\xi}\left[\int\frac{\eta\,d\eta}{\left(1+\frac{\nu_t}{\nu}\frac{\mathrm{Pr}}{\mathrm{Pr}_t}\right)}-\int\frac{d\eta}{\left(1+\frac{\nu_t}{\nu}\frac{\mathrm{Pr}}{\mathrm{Pr}_t}\right)}\right]. \tag{18}$$

We give the turbulence function in the film in the form (3)

$$\frac{\nu_t}{\nu}=\varepsilon_m\eta^2\left(1-\eta^2\right), \tag{19}$$

where $\varepsilon_m = 5\cdot 10^{-5}\,\mathrm{Re}^{1,4}\left\{1+3,6\left[1-\exp\left(1-\frac{d}{d_o}\right)\right]\right\}\left[1-0,1\exp\left(-1,1086\sqrt{We}\right)\right]C_u$.

Provided that $\Pr_t = 1$, expression (18) taking into account (19) will be rewritten as

$$\theta(\eta,\xi) = \frac{Pe}{4}\frac{\partial\theta_{av}(\xi)}{\partial\xi}\left[\int\frac{\eta\, d\eta}{\left(1+\varepsilon_m\left(\eta^2-\eta^4\right)\Pr\right)} - \int\frac{d\eta}{\left(1+\varepsilon_m\left(\eta^2-\eta^4\right)\Pr\right)}\right],$$

and its integration under boundary conditions $\eta = 0$, $\theta = 1$ gives

$$\theta(\eta,\xi) = 1+\frac{Pe}{4}\frac{\partial\theta_{av}(\xi)}{\partial\xi}\left[\begin{array}{l}\frac{1}{H}Arth\left(\frac{P\left(2\eta^2-1\right)}{H}\right)+\frac{\sqrt{2}H}{(4+P)A}Arth\left(\frac{\sqrt{2}P}{A}\eta\right)- \\ -\frac{\sqrt{2}H}{(4+P)B}Arth\left(\frac{\sqrt{2}P}{B}\eta\right)+\frac{1}{H}Arth\left(\frac{P}{H}\right)\end{array}\right], \qquad (20)$$

where $H = \sqrt{4P+P^2}$; $A = \left[P-\left[P(4+P)\right]^{1/2}P\right]^{1/2}$; $B = \left[P+\left[P(4+P)\right]^{1/2}P\right]^{1/2}$; $P = \varepsilon_m \Pr$.

The derivative $\frac{\partial\theta_{av}(\xi)}{\partial\xi}$ is unknown. The average temperature, which is included in equation (20) and which is subject to determination, is defined as average mass

$$\theta_{av} = \int_0^1 \theta(\eta,\xi)\frac{u(\eta)}{\bar{u}}d\eta = \int_0^1 \frac{6}{5}\eta^{\frac{1}{5}}\theta(\eta,\xi)d\eta\ . \qquad (21)$$

There is no analytical expression for the integral (21), but assuming the fullness of the velocity profile, with a certain approximation with respect to the average temperature $\theta_{av}(\xi)$, we apply the simplification

$$\theta_{av}(\xi) = \int_0^1 \theta(\eta,\xi)\frac{u(\eta)}{\bar{u}}d\eta \approx \int_0^1 \theta(\eta,\xi)d\eta\ . \qquad (22)$$

Then as a result of integration (22) we get:

$$\theta_{av}(\xi)=1+\frac{Pe}{4}\frac{\partial\theta_{cp}}{\partial\xi}\left[\begin{array}{l}\frac{H}{2P(P+4)}\ln\left(\frac{A^2-2P^2}{B^2-2P^2}\right)+\frac{2}{H}Arth\left(\frac{P}{H}\right)+\\+\frac{\sqrt{2}(P-H)}{2aH}Arth\left(\frac{\sqrt{2}P}{a}\right)-\frac{\sqrt{2}}{2}\frac{(P+H)}{bH}Arth\left(\frac{\sqrt{2}P}{b}\right)+\\+\frac{\sqrt{2}H}{(P+4)}\left(\frac{1}{A}Arth\left(\frac{\sqrt{2}P}{A}\right)-\frac{1}{B}Arth\left(\frac{\sqrt{2}P}{B}\right)\right)+\frac{H}{P(4+P)}\ln\left(\frac{B}{A}\right)\end{array}\right],$$

where $a=\sqrt{P^2-PH}$; $b=\sqrt{P^2+PH}$.

Denoting the expression in square brackets as

$$S=\frac{Pe}{4}\left[\begin{array}{l}\frac{H}{2P(P+4)}\ln\left(\frac{A^2-2P^2}{B^2-2P^2}\right)+\frac{2}{H}Arth\left(\frac{P}{H}\right)+\\+\frac{\sqrt{2}(P-H)}{2aH}Arth\left(\frac{\sqrt{2}P}{a}\right)-\frac{\sqrt{2}}{2}\frac{(P+H)}{bH}Arth\left(\frac{\sqrt{2}P}{b}\right)+\\+\frac{\sqrt{2}H}{(P+4)}\left(\frac{1}{A}Arth\left(\frac{\sqrt{2}P}{A}\right)-\frac{1}{B}Arth\left(\frac{\sqrt{2}P}{B}\right)\right)+\frac{H}{P(4+P)}\ln\left(\frac{B}{A}\right)\end{array}\right],$$

we come to the differential equation

$$\theta_{av}=1+S\frac{d\theta_{av}}{d\xi},$$

solution of which, under the initial condition $\xi=0$; $\theta=0$, gives an expression for the average temperature

$$\theta_{av}=\left[1-\exp\left(\frac{\xi}{S}\right)\right].$$

Derivative from θ_{av} to ξ

$$\frac{d\theta_{av}}{d\xi}=-\frac{1}{S}\exp\left(\frac{\xi}{S}\right).$$

By substituting the obtained derivative into the original equation, we obtain the limiting curve $\theta_m(\eta,\xi_m)$ at the distance ξ_m, at which the condition $\frac{\partial\theta}{\partial\eta}=0$

$$\theta_m(\eta,\xi_m)=1-\frac{Pe}{4S}\exp\left(\frac{\xi_m}{S}\right)\left[\begin{array}{l}\frac{1}{H}Arth\left(\frac{P\left(2\eta^2-1\right)}{H}\right)+\frac{\sqrt{2}H}{(4+P)A}Arth\left(\frac{\sqrt{2}\,P}{A}\eta\right)-\\ -\frac{\sqrt{2}H}{(4+P)B}Arth\left(\frac{\sqrt{2}\,P}{B}\eta\right)+\frac{1}{H}Arth\left(\frac{P}{H}\right)\end{array}\right] \quad (23)$$

A graphic representation of the obtained function $\theta_m(\eta,\xi_m)$ is shown in Figure 5.

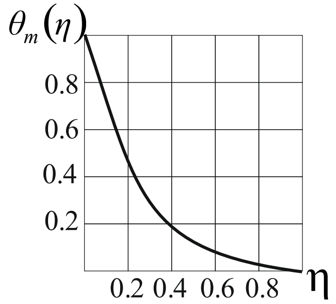

Figure 5. Graphic representation of the limiting temperature curve (23) from the dimensionless transverse coordinate $\theta_m = f(\eta)$ with the parameters:
$P=10$, $Pe=12000$.

The coordinate ξ_m for which $\frac{\partial\theta}{\partial\eta}=0$ is found from the condition $\eta=1$, $\theta(1,\xi_m)=0$

$$0=1-\frac{Pe}{4S}\exp\left(\frac{\xi_m}{S}\right)\left[\begin{array}{l}\frac{1}{H}Arth\left(\frac{P}{H}\right)+\frac{\sqrt{2}H}{(4+P)A}Arth\left(\frac{\sqrt{2}\,P}{A}\right)-\\ -\frac{\sqrt{2}H}{(4+P)B}Arth\left(\frac{\sqrt{2}\,P}{B}\right)+\frac{1}{H}Arth\left(\frac{P}{H}\right)\end{array}\right].$$

Denoting the expression in square brackets as K

$$K=\left[\begin{array}{l}\frac{1}{H}Arth\left(\frac{P}{H}\right)+\frac{\sqrt{2}H}{(4+P)A}Arth\left(\frac{\sqrt{2}\,P}{A}\right)-\\ -\frac{\sqrt{2}H}{(4+P)B}Arth\left(\frac{\sqrt{2}\,P}{B}\right)+\frac{1}{H}Arth\left(\frac{P}{H}\right)\end{array}\right],$$

we will get the ratio for calculation ξ_m in the turbulent mode of motion of the film

$$\xi_m = S\ln\left(\frac{4S}{Pe\,K}\right). \quad (24)$$

The graphical interpretation of (24) is shown in Figure 6.

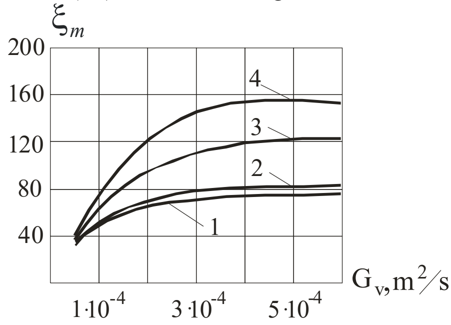

Figure 6. Dependence of the dimensionless ξ_m length overcome by a turbulent film, at which the heat transfer regimes to the film change from the volumetric liquid flux G_v:
1 – free flow;
u, m/s: 2 – 15 *m/s*; 3 – 25; 4 – 35.

To obtain the physical length of the boundary of the zones x_m under the turbulent regime, it is necessary to determine the thickness of the film from the equation of motion using the dependence for turbulent viscosity (3)

$$\frac{\tau_i\delta}{\rho\nu}+\frac{g\delta^2}{\nu}(1-\eta)=\left[1+\varepsilon_m\left(\eta^2-\eta^4\right)\right]\frac{du}{d\eta}. \tag{25}$$

From (25) under boundary conditions $\eta = 0,\ u = 0$, we obtain the velocity profile

$$u=\left(\frac{\tau_i\delta}{\rho\nu}+\frac{g\delta^2}{\nu}\right)\frac{\sqrt{2}h}{(4+\varepsilon_m)}\left[\frac{1}{r}Arth\left(\frac{\sqrt{2}\varepsilon_m}{r}\eta\right)-\frac{1}{j}Arth\left(\frac{\sqrt{2}\varepsilon_m}{j}\eta\right)\right]-$$
$$-\frac{g\delta^2}{\nu h}\left[Arth\left(\frac{\varepsilon_m\left(2\eta^2-1\right)}{h}\right)+Arth\left(\frac{\varepsilon_m}{h}\right)\right], \tag{26}$$

Where $h=\sqrt{4\varepsilon_m+\varepsilon_m^2}$; $j=\sqrt{\varepsilon_m^2-\varepsilon_m h}$; $r=\sqrt{\varepsilon_m^2+\varepsilon_m h}$;

$$n=\left[\frac{1}{r}Arth\left(\frac{\sqrt{2}\,\varepsilon_m}{r}\right)-\frac{1}{j}Arth\left(\frac{\sqrt{2}\,\varepsilon_m}{j}\right)\right].$$

The average speed $\bar{u}=\int_0^1 u\,d\eta$ is obtained from (26):

$$\bar{u}=\left(\frac{\tau_i\delta}{\rho\nu}+\frac{g\delta^2}{\nu}\right)\frac{\sqrt{2}h}{(4+\varepsilon_m)}\left[n-\frac{\sqrt{2}}{4\varepsilon_m}\ln\left(\frac{j^2-2\varepsilon^2}{r^2-2\varepsilon^2}\right)-\frac{\sqrt{2}}{2\varepsilon_m}\ln\left(\frac{r}{j}\right)\right]-$$
$$-\frac{g\delta^2}{\nu h}\left[2Arth\left(\frac{\varepsilon_m}{h}\right)-\frac{\sqrt{2}h}{2}\left(\frac{1}{r}Arth\left(\frac{\sqrt{2}\varepsilon_m}{r}\right)+\frac{1}{j}Arth\left(\frac{\sqrt{2}\varepsilon_m}{j}\right)\right)-\frac{\sqrt{2}\varepsilon_m}{2}n\right]. \tag{27}$$

The thickness of the film δ and the average speed $\bar{u}$ are related to the volumetric liquid flux G_v by dependence $\delta = \frac{G_v}{\bar{u}}$. Whence the expression for the average thickness of the film takes the form of a cubic equation

$$G_v = \left(\frac{\tau_i \delta^2}{\rho \nu}\right) D + \frac{g\delta^3}{\nu h}\left(D h - B\right), \tag{28}$$

where

$$B = \left[2Arth\left(\frac{\varepsilon_m}{h}\right) - \frac{\sqrt{2}h}{2}\left(\frac{1}{r}Arth\left(\frac{\sqrt{2}\varepsilon_m}{r}\right) + \frac{1}{j}Arth\left(\frac{\sqrt{2}\varepsilon_m}{j}\right)\right) - \frac{\sqrt{2}\varepsilon_m}{2}n\right],$$

$$D = \frac{\sqrt{2}h}{\left(4+\varepsilon_m\right)}\left[n - \frac{\sqrt{2}}{4\varepsilon_m}\ln\left(\frac{j^2 - 2\varepsilon_m^2}{r^2 - 2\varepsilon_m^2}\right) - \frac{\sqrt{2}}{2\varepsilon_m}\ln\left(\frac{r}{j}\right)\right].$$

In the case of free flow ($\tau_i = 0$), the film thickness is directly from (28)

$$\delta = \sqrt[3]{\frac{G_v \nu h}{g\left(Dh - B\right)}}. \tag{29}$$

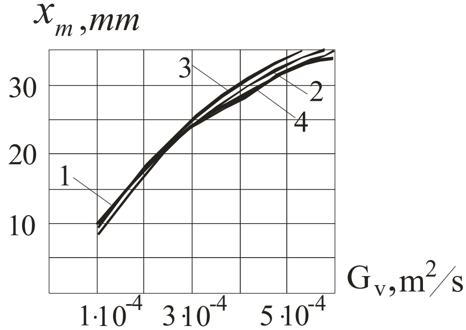

Figure 7. Dependence of the physical x_m length overcome by a turbulent film, at which the heat transfer regimes to the film change from the volumetric liquid flux G_v:
1 – free flow; u_2, *m/s:* 2 – 15; 3 – 25; 4 – 35.

Regarding the distance covered by the film during the period between the passage of two large waves. The phase speed of the large wave c exceeds the average speed of the film $\bar{u}$, so a selected section of the film moving at speed $\bar{u}$ will be crossed by the next wave in time τ at a distance of x.

$$\tau = \frac{\lambda_{bw}}{c - \bar{u}},$$

where c, λ_{bw} – face velocity and length of large waves, respectively.

The distance x covered by the film in time τ, moving at speed $\bar{u}$, between the crests of large waves is equal to

$$x = \bar{u}\tau = \frac{\bar{u}\lambda_{bw}}{c-\bar{u}} = \frac{\bar{u}c}{f_{bw}\left(c-\bar{u}\right)} = \frac{c}{f_{bw}\left(\frac{c}{\bar{u}}-1\right)} \quad , \tag{30}$$

where f_{bw} – is the frequency of large waves. The quantities c, λ_{bw}, f_{bw} are functions of irrigation density, interfacial tangential stress, and channel geometry. According to data known from the literature, the phase speed exceeds the average speed of the film by 2.5– 1.5 times, and the length of large waves λ_{bw} in long pipes is 100–140 mm, depending on the density of irrigation. If we take the average value of the phase speed $c = 2\bar{u}$, we get the distance covered by the film during the passage of two large waves, which, according to (30), is equal to the wavelength of $x \cong \lambda_{bw}$. Thus, since $x_m \le \lambda_{bw}$ two modes of heat exchange are realized during a wave cycle on the entire gap of the film surface between two large waves. The initial condition for finding the temperature profile in the second period is equation (12) for laminar and (23) for turbulent film motion modes.

Conclusions

1. The obtained relations (13) for the laminar flow and (24) for the turbulent flow allow us to calculate the length of the film movement between two large waves up to the limit ($\xi = \xi_m$), at which the character of the heat transfer to the boiling film changes – from the heating mode to the saturation state on the interfacial surface to the evaporation mode with of the interfacial surface with an increase in the heat flux in the process of movement to the steady state.
2. As a result of solving the convective heat conduction equation with the boundary conditions $\eta = 0$, $\theta = 1$; $\eta = 1$, $\frac{\partial \theta}{\partial \eta} = 0$ and the initial condition: $\xi = 0$, $\theta_{av} = 0$, obtained solutions for laminar (12) and turbulent (23) flows, which are the initial conditions for the equation of convective heat conduction in the second period of development of the temperature field in the film at $\xi = \xi_m$.
3. The parameter x_m for the turbulent flow is not very sensitive to changes in the velocity of the vapor core, since as the film thickness decreases due to the dynamic action of the flow core on the film, the intensity of turbulence in the film also decreases.

References

Demekhin E.A., Kalaidin E.N., Rastarukhin A.A. (2005), Influence of wave regimes on mass transfer in falling liquid films, *Thermophysics and Aeromechanics*, 12(2), pp. 259–269.

Dietze G.F. (2016), On the Kapitza instability and the generation of capilary waves, *Journal of Fluid Mechanics,* 789, pp. 368–401, https://doi.org/10.1017/jfm.2015.736

Dietze G.F., Rohlfs W., Kneer R. (2014), Three-dimensional flow structures in laminar liquid films, *Journal of Fluid Meghanics*, 743, pp. 75–123, https://doi.org/10.1017/S0022112009008155

Gourdon M., Karlsson E., Innings A., Vamling L. (2015), Heat transfer for falling film evaporation of indastrially revevant fluids up to very high Prandtl numbers, *Heat and Mass Transfer*, 52(2), pp. 379–391.

Kostoglou M., Samaras K., Karapantsios T.D. (2010), Large wave characteristics and their downstream evolution at high reynolds number falling films, *AICHE Journal,* 56(1), pp. 11–23.

Lel V.V., Al-Sibai F., Kneer R. (2009), Thermal Entry Length and Heat ransfer Phenomena in Laminar Wavy Falling Films, *Microgravity Science and Technology*, 21(S1), pp. 215 – 220

Malamataris N.A., Balakotaiah V. (2008), Flow structure unerneath the larg amplitude waves of a vertically falling film*, AIChE Journal*, 54(7), pp. 1725–1740.

Mascarenhas N., Mudawar I. (2013), Investigation of eddy diffusivity and hea transfer coefficient for free-falling turulent liquid films subjected to sensible heating, *International Journal of Heat and Mass Transfer,* 64, pp. 647–660, https://doi.org/10.1016/j.ijheatmasstransfer.2013.04.061

Mascarenhas N., Mudawar I. (2013), Stady of the influencial waves on heat transfer in turbulent falling films, *International Journal of Heat and Mass Transfer*, 67, pp. 1106–1121, https://doi.org/10.1016/j.ijheatmasstransfer.2013.08.100

Petrenko V., Pryadko M., Ryabchuk O. (2020), Modeling heat transfer in down flowing annular weakly tyrbulent vapor-liquid flows during evaporation, *Ukrainian Food Journal*, 9(4), pp. 901–916, https://doi.org/10.24263/2304-974X-2020-9-4-14